



Published in final edited form as:

*J Med Chem.* 2011 August 25; 54(16): 5858–5867. doi:10.1021/jm200591t.

## Fluorescent Derivatives of $\sigma$ Receptor Ligand 1-Cyclohexyl-4-[3-(5-methoxy-1,2,3,4-tetrahydronaphthalen-1-yl)propyl]piperazine (PB28) as a Tool for Uptake and Cellular Localization Studies in Pancreatic Tumor Cells

Carmen Abate<sup>†,\*</sup>, John R. Hornick<sup>§</sup>, Dirk Spitzer<sup>§</sup>, William G Hawkins<sup>§</sup>, Mauro Niso<sup>‡</sup>, Roberto Perrone<sup>‡</sup>, and Francesco Berardi<sup>‡</sup>

<sup>‡</sup>Dipartimento Farmacochimico, Università degli Studi di Bari ALDO MORO, Via Orabona 4, I-70125 Bari, Italy

<sup>§</sup>Division of Hepatobiliary, Pancreatic, and Gastrointestinal Surgery, Department of Surgery, Washington University School of Medicine, St. Louis, MO

### Abstract

Fluorescent derivatives of  $\sigma_2$  high affinity ligand 1-cyclohexyl-4-[3-(5-methoxy-1,2,3,4-tetrahydronaphthalen-1-yl)propyl]piperazine **1** (PB28) were synthesized. NBD or Dansyl fluorescent tags were connected through a 5- or 6-atoms linker in two diverse positions of **1** structure. Good  $\sigma_2$  affinities were obtained when the fluorescent tag was linked to 5-methoxytetralin nucleus replacing the methyl function. NBD-bearing compound **16** displayed high  $\sigma_2$  affinity ( $K_i = 10.8$  nM) and optimal fluorescent properties. Its uptake in pancreatic tumor cells was evaluated by flow cytometry showing that it partially occurs through endocytosis. In proliferating cells the uptake was higher supporting that  $\sigma_2$  receptors are markers of cell proliferation and that the higher is the proliferation, the stronger is the antiproliferative effect of  $\sigma_2$  agonists. Colocalization of **16** with subcellular organelles was studied by confocal microscopy: the greatest was in endoplasmic reticulum and lysosomes. Fluorescent  $\sigma_2$  ligands show their potential in clarifying the mechanisms of action of  $\sigma_2$  receptors.

### Introduction

After their first discovery in 1976, sigma ( $\sigma$ ) receptor research met a renovated enthusiasm in the early 1990's when the two subtypes,  $\sigma_1$  and  $\sigma_2$ , were identified.<sup>1</sup> The  $\sigma_1$  subtype was soon thereafter isolated and cloned from different sources,<sup>2</sup> and it has been recently classified as a receptor chaperone at the endoplasmic reticulum (ER) membrane that regulates ER-mitochondrial  $\text{Ca}^{2+}$  signalling and cell survival.<sup>3</sup> Though their mechanism of action is still unclear,  $\sigma$  proteins receive much interest because of their potential applications as drug targets for a wide range of diseases.  $\sigma_1$  Receptor ligands display neuroprotective and neuroregulative functions and are under evaluation for the treatment of a number of neurological disorders<sup>4</sup> such as depression,<sup>5</sup> schizophrenia,<sup>6</sup> Alzheimer's and Parkinson's diseases<sup>7-9</sup> and for drug abuse (e.g., cocaine).<sup>10</sup> The high therapeutic potential of  $\sigma_2$  receptors comes from the evidence that this subtype is overexpressed in a wide variety of cancer tissues, and activation of  $\sigma_2$  receptors lead tumor cells to death through different

<sup>†</sup>To whom correspondence should be addressed. Tel.: +39-080-5442748. Fax.: +39-080-5442231. abate@farmchim.uniba.it.

**Supporting Information Available:** Elemental analyses of the novel end products; Formulas, melting points of hydrochloride salts; fluorescence microscopy images taken with compound **16** and subcellular organelles trackers. This material is available free of charge via the Internet at <http://pubs.acs.org>.

apoptotic pathways.<sup>11-13</sup> Therefore, a number of  $\sigma_2$  receptor ligands are under investigation for cancer treatment and diagnosis.<sup>14-16</sup> Nevertheless, the  $\sigma_2$  subtype is not as well as characterized as the  $\sigma_1$ . It has not yet been cloned and attempted characterization from homogenate of  $\sigma_2$ -overexpressing tumor cells led to isolation of histone proteins by affinity chromatography.<sup>17</sup> The  $\sigma_2$  selector used was a derivative of 1-cyclohexyl-4-[3-(5-methoxy-1,2,3,4-tetrahydronaphthalen-1-yl)-*n*-propyl]piperazine (**1**, PB28), one of the highest affinity  $\sigma_2$  receptor ligands known<sup>18,19</sup> concluding that either  $\sigma_2$  receptors may be histones or histone binding proteins or compound **1** binds such proteins as well as  $\sigma_2$  receptors, with modeling studies conducted to rationalize these hypotheses.<sup>20</sup> Such results were in disagreement with findings from fluorescence microscopy, which localizes  $\sigma_2$  subtypes in several organelles except the nucleus through the use of fluorescent  $\sigma_2$  ligands.<sup>21,22</sup> Besides the intracellular localization, there are other ambiguities related to the  $\sigma_2$  receptors: evidence shows that  $\sigma_2$  ligands activate different apoptotic pathways in diverse tumor cells.<sup>11-13,23</sup> With the aim of helping to clarify some of these ambiguities, we synthesized a small series of fluorescent derivatives of compound **1** to be used in microscopy studies for the purpose of localizing  $\sigma_2$  receptors subcellularly within cancer cells.

Intrinsically fluorescent compound **1** analogues have been synthesized in the past, with appreciable  $\sigma$  receptor affinity but with maximum excitation and emission wavelength ( $\lambda_{exc}$  and  $\lambda_{em}$ ) inappropriate for use in living cells for fluorescence microscopy.<sup>24</sup> Therefore, we followed a common approach to overcome this limitation: dansyl ( $\lambda_{exc}$  ~315 nm) and 7-nitro-2,1,3-benzoxadiazole (NBD) ( $\lambda_{exc}$  ~420 nm) moieties were alternatively inserted in two different positions on compound **1** structure through a 5- or 6-atoms linker. Such separation between the pharmacophore and the fluorescent tag should prevent the loss of affinity leaving the fluorescent properties of the fluorescent moieties almost unchanged. Compound **16**, with the best fluorescence/pharmacological properties, was used for preliminary fluorescence microscopy analyses in murine and human pancreatic tumor cells which have been previously shown to overexpress  $\sigma_2$  receptors.<sup>11</sup> Human pancreatic tumor cells (BxPC3) were selected for more extensive studies of compound **16** whose internalization and colocalization by confocal microscopy with subcellular organelles were evaluated.

## Results and Discussion

### Chemistry

The synthetic pathways for final compounds **7**, **8**, **16-19** are depicted in Scheme 1 and 2. Key intermediate **6** was prepared starting from commercial piperidin-4-one ethylene ketal (1,4-dioxo-8-aza-spiro[4.5]decane) which was alkylated with 6-bromohexanenitrile affording intermediate **2**. Upon reduction with  $\text{LiAlH}_4$  to the corresponding amine and subsequent amine-protection through acetylation, compound **2** provided derivative **3**. Acidic deprotection of the ethylene-acetal function with HCl led to intermediate **4** which underwent reductive amination with piperazine **5**<sup>25</sup> providing the acetyl derivative of **6**, which was deacetylated affording key amine **6**. Reaction of this latter alternatively with NBD-chloride or dansyl chloride afforded the fluorescent compounds **7** and **8** respectively (Scheme 1).

The final compounds **16-19** were synthesized as outlined in Scheme 2. The reaction between potassium phthalimide and 1,6-dibromohexane gave intermediate **9**<sup>26</sup> which was used to alkylate the key phenolic intermediate **10**<sup>19</sup> affording phthalimide **11**. Alkylation of the phenolic intermediate **9** with 2-(2-chloroethoxy)ethanol afforded the corresponding alcohol **12** that underwent Mitsunobu condensation with phthalimide in the presence of triphenylphosphine and diisopropylazodicarboxylate (DIAD) to yield compound **13**. Phthalimide derivatives **11** and **13** underwent hydrazinolysis to afford intermediate primary

amines **14** and **15** respectively. Reaction of **14** with NBD-chloride or dansyl chloride afforded the fluorescent compounds **16** and **18** respectively. Reaction of **15** with NBD-chloride or dansyl chloride afforded respectively the fluorescent final compounds **17** and **19**. All the final compounds were converted to the corresponding hydrochloride salts with gaseous HCl.

### Radioligand Binding and $\sigma_1$ and $\sigma_2$ Receptor Affinities

Results from binding assays are expressed as inhibition constants ( $K_i$  values) in Table 1. The introduction of the fluorescent tag and the linker produced a decrease in the affinity at both  $\sigma$  receptors with respect to lead compound **1**. The most dramatic drop in the affinity at both  $\sigma$  receptors was observed with compounds **7** ( $K_i = 2570$  nM for  $\sigma_1$  and  $K_i = 1720$  nM for  $\sigma_2$  receptor), and **8** ( $K_i > 5000$  nM for  $\sigma_1$  and  $K_i = 5020$  nM for  $\sigma_2$  receptor) which reached micromolar values. In such compounds the piperidine ring replacing the cyclohexyl ring was functionalized with the fluorescent tag through a six-methylene chain. The drop in the affinity was independent from the nature of the fluorescent tag indicating that functionalization (at least with a six-atom linker) in that position of the pharmacophore was not tolerated by the  $\sigma_2$  receptors, in accordance with a previous study in which substitution of the cyclohexyl with more hindered substituents led to reduced  $\sigma$  affinities.<sup>18,27</sup> On the other hand, fluorescent final compounds obtained through insertion of the alkyl fluorescent tag on the 5-methoxy-tetralin ring in place of the methyl group, displayed nanomolar affinities at both  $\sigma$  receptors (compounds **16-19**). Previous SAfiR studies demonstrated how the methoxy substituent was unessential for  $\sigma_2$  receptor binding indeed.<sup>28</sup> NBD or Dansyl moieties were tolerated at the  $\sigma_2$  receptor with the highest affinity displayed by the NBD-bearing compound **16** ( $K_i$ s = 10.8 nM). The presence of the NBD, but not of the dansyl moiety, appeared to be detrimental ( $K_i = 78.8$  nM for **16** and  $K_i = 96.2$  nM for **17**) for  $\sigma_1$  receptor binding. With  $\sigma_1$  and  $\sigma_2$  affinities in the same range, dansyl-bearing ligands **18** and **19** did not show any  $\sigma_2$  versus  $\sigma_1$  selectivity, whereas compounds bearing NBD (**16** and **17**) displayed a moderate  $\sigma_2$  selectivity (8-fold and 2.5-fold respectively). Selectivity was missing in lead compound **1** when binding assays were performed on animal tissues according to literature protocols.<sup>18</sup> Results obtained with this small series of compounds demonstrated that a fluorescent tag spaced out from the tetralinoxy moiety by a 5- or 6-atom linker leads to molecules with good  $\sigma$  receptor affinities useful for in living cells visualization of  $\sigma_2$  receptors, with compound **16** displaying the best pharmacological properties for further investigation.

### Fluorescent Ligand Studies

The fluorescent properties of final compounds are listed in Table 1. The excitation and emission spectra were obtained from solution of the final compounds in organic solvents (EtOH and  $\text{CHCl}_3$ ) and in aqueous solution (PBS buffer). The NBD-bearing compounds (**8**, **16**, **17**) displayed excitation peaks at two different wavelengths ( $\sim 335$  nm and  $\sim 450$  nm) and for both the wavelengths, the corresponding  $\lambda_{em}$  was  $\sim 520$  nm. The  $\lambda_{exc}$  selected to perform the assays in living cells was 450 nm to avoid cells autofluorescence phenomena. Dansyl-bearing compounds (**7**, **18**, **19**) displayed a  $\lambda_{exc}$  more shifted toward the UV region ( $\sim 340$  nm). All of the compounds showed an important difference between  $\lambda_{exc}$  and  $\lambda_{em}$  (Stokes shift). Quantum yields ( $\Phi$ ) were determined in the above mentioned solvents to probe the environment affecting the sensitivity of the final fluorescent ligands, since the fluorophores selected (Dansyl and NBD) are endowed with environment sensitivity properties, (i.e. low quantum yield in aqueous solution but high fluorescence in nonpolar solvents or when bound to a hydrophobic sites). All tested compounds exhibited very low fluorescence in PBS buffer but became fluorescent in the organic solvents. The highest quantum yields were those recorded in  $\text{CHCl}_3$  for all the final compounds:  $\Phi$  values were 2- or 4-fold higher in  $\text{CHCl}_3$  than in EtOH for NBD-bearing compounds (**8**, **16**, **17**) and several

fold higher than in PBS buffer. Dansyl-bearing compounds (**7**, **18**, **19**) showed a less pronounced increase in  $\Phi$  values from EtOH to CHCl<sub>3</sub> solutions, although the highest  $\Phi$  was shown by compound **19** ( $\Phi = 0.48$ ). Molar extinction coefficients ( $\epsilon$ ) were determined for all final compounds (in EtOH), with the lowest values displayed by the dansyl-bearing compounds (2600-4000 L/mol-cm) and the highest values displayed by the NBD-bearing compounds (6544-14391 L/mol-cm) indicating that the fluorescence intensity of the latter compounds is stronger. Preliminary fluorescence microscopy experiments were conducted with compound **16** which displayed the best combination between pharmacological ( $\sigma_2$  receptor affinity and selectivity) and fluorescence properties (convenient excitation and emission wavelengths and high  $\epsilon$  value) and promising results were obtained in different tumor pancreatic cells which were previously shown to overexpress  $\sigma_2$  receptors.<sup>11</sup> Therefore, compound **16** was evaluated in more details in *in vitro* internalization studies and cellular colocalization by confocal microscopy in human pancreatic tumor cells (BxPC3).

### In vitro Internalization Studies

Uptake of compound **16** in BxPC3 pancreatic cancer cells was analyzed immediately following treatment (25 nM) and the mean fluorescence recorded over time (Figure 1A). The  $T_{1/2}$  of maximum fluorescence at 60 min was  $7.8 \pm 1.5$  min (mean  $\pm$  SEM). We further studied uptake for the purpose of better understanding the involvement of endocytosis of these compounds and the receptor. Caveolin-mediated (lipid rafts-mediated) endocytosis can be inhibited by Filipin III<sup>29</sup> and clathrin-mediated endocytosis by phenylarsine oxide (PAO).<sup>30</sup> BxPC3 cells were pretreated with Filipin III (5  $\mu$ g/mL) or PAO (10 mM) for 30 min prior to treatment with compound **16** (25 nM) and mean fluorescence was collected over 60 min. The rate of uptake was decreased from  $7.8 \pm 1.5$  min to  $6.8 \pm 0.8$  min for Filipin III and  $4.9 \pm 2.1$  min for PAO. As well, the overall uptake at 60 min was decreased to 69% and 50% for Filipin III and PAO respectively. Taken together, the  $T_{1/2}$  in the range of min and the decreased uptake in the presence of endocytosis inhibitors, suggest that the internalization of **16** occurs, in part, through the caveolin- and clathrin-mediated endocytotic pathways in addition to simple membrane diffusion. Uptake by the clathrin-dependent pathway has been described previously with other  $\sigma_2$  receptor ligands,<sup>21,22</sup> but uptake by the caveolin-dependent/lipid raft pathway has not been previously reported. Interaction and endocytosis of compound **16** through lipid rafts is of note considering that  $\sigma_2$  receptor agonists were initially found to bind to protein constituents of the lipid rafts,<sup>31,32</sup> cholesterol-rich domains in the cell membrane. They form flask shaped invaginations called caveolae, for the caveolin protein that coats them, and act as platforms for glycosphosphatidylinositol-linked protein mediated signaling pathways and internalization of cholesterol.<sup>33</sup> Interest has grown in targeting this pathway in cancer cells, which may have disrupted lipid rafts contributing to aberrances in pathways implicated in chemoresistance such as the epidermal growth factor receptor and tumor necrosis factor alpha receptor.<sup>34</sup>

Therefore, implication of lipid raft disruption in oncology signaling and response to chemotherapy together with the presence of  $\sigma_2$  proteins in lipid rafts suggest that  $\sigma_2$  receptor mediated toxicity and chemoresistance overcome (which has been shown with different  $\sigma_2$  receptor agonists),<sup>23,35</sup> likely involve lipid rafts.

In vitro competition was performed to quantify interaction of compound **16** with  $\sigma_2$  agonists in the live cell. Preloading with **1** or the recently produced  $\sigma_2$  agonist *cis*-1-cyclohexyl-4-[4-(2,6-difluorophenyl)cyclohexyl]piperazine<sup>36</sup> (**20**) for 45 min prior to addition of compound **16** for 45 min decreased the mean fluorescence intensity of **16** with increasing concentrations of  $\sigma_2$  agonist (Figure 1B). This indicates that the fluorescent compound functionally competes for localization in the same plane as the parent and analog compound.

The correlation between the proliferative status of tumors and the expression of the  $\sigma_2$  receptors has been widely demonstrated in different cancer cell lines,<sup>22,37,38</sup> and we have further detailed the expression and apoptosis response in pancreatic cancer cells.<sup>11,39</sup> In this study, we further evaluated the impact of proliferation on  $\sigma_2$  agonist uptake and sensitivity (Figure 1C). In order to maintain proliferating versus quiescent cell cultures, subcultured cells were seeded at increasing densities in order to achieve subconfluent and confluent cultures respectively. Compound **16** mean fluorescence at 30 min decreased as cell density increased, in accordance with earlier findings that  $\sigma_2$  receptors are markers of cell proliferation.<sup>40</sup> In addition, the decreased uptake was associated with decreased cell death as the density increased, so that the reduction of the antiproliferative activity of  $\sigma_2$  agonists **1** and **20** was likely due to the  $\sigma_2$  reduced presence in non proliferating cells. Together, these findings show that compound **16** performs biologically as expected for a  $\sigma_2$  ligand, and that increased uptake of  $\sigma_2$  agonists by proliferating cells is a critical step for mediating cell death.

Cellular colocalization studies of these fluorescent analogs of **1** were initially screened by epifluorescent microscopy (supplementary information), and confocal microscopy results were in accordance with those findings (Figure 2). BxPC3 cells were incubated with fluorescent ligand **16** and MitoTracker Red, ERTracker Red, LysoTracker Red, or Vybrant cholera-toxin B subunit (CT-B), at 37 °C for 30 min prior to fixation and nuclear staining with TO-PRO-3. Compound **16** is found in the membrane fractions of the cell, and colocalizes greatest in the endoplasmic reticulum and lysosomes, with moderate colocalization in the mitochondria and the plasma membrane (CT-B). Colocalization in the nucleus was not observed with TO-PRO-3.

## Conclusions

Fluorescent  $\sigma_2$  ligands were obtained linking dansyl or NBD moieties in two different positions of compound **1** structure. High affinity  $\sigma_2$  ligands were obtained when the fluorescent tag was attached on the tetralin ring through an alkyl linker replacing the methyl in the methoxy function. On the other hand, the approach of attaching a fluorescent tag at the compound **1** cyclohexyl moiety -replaced by a piperidine ring- was unsuccessful, and a dramatic drop in the affinity was recorded. NBD-bearing compounds displayed better fluorescent properties (more convenient  $\lambda_{exc}$  and  $\lambda_{em}$  and high fluorescence intensity) than dansyl-bearing compounds, and among them, compound **16** displayed high  $\sigma_2$  receptor affinity and moderate  $\sigma_1/\sigma_2$  selectivity. Therefore, compound **16** internalization was studied by flow cytometry and by confocal microscopy for colocalization with subcellular organelles in BxPC3 pancreatic tumor cells. The uptake of fluorescent ligand **16** decreased in the presence of non-fluorescent  $\sigma_2$  ligands showing that fluorescent and non-fluorescent compounds compete for localization in the same plane. Endocytosis inhibitors decreased the uptake of compound **16** showing that internalization occurs, in part, through endocytotic pathways besides simple membrane diffusion, and that interaction with lipid rafts, which may be able to influence the membrane composition and downstream signalling, takes place, so that  $\sigma_2$  receptor mediated toxicity and chemoresistance overcome likely involve lipid rafts. The influence of proliferation, with cell density as a surrogate, on  $\sigma_2$  agonist uptake and sensitivity was studied and showed that the uptake is higher in proliferating cells, supporting that  $\sigma_2$  receptors are markers of cell proliferation.<sup>37,38</sup> Furthermore, the sensitivity of BxPC3 cells for  $\sigma_2$  agonists decreased together with the uptake, as the density (i.e. quiescent cells) increased, suggesting that uptake is a critical step for mediating  $\sigma_2$  agonists-dependent cell death. Compound **16** colocalized to the greatest extent in the endoplasmic reticulum and lysosomes, with moderate colocalization in the mitochondria and the plasma membrane, but no colocalization in the nucleus was observed in disagreement with the histone hypothesis which will have to be further analyzed.



All in all, it was demonstrated that the use of fluorescent  $\sigma_2$  ligands may help in clarifying the mechanisms of action of the still enigmatic  $\sigma_2$  receptors. The use of such compounds in different cell lines, may contribute to understand the different cell type apoptotic pathways activated by  $\sigma_2$  ligands. Furthermore, a scaffold which appears optimal for inferring high  $\sigma$  receptor affinities was herein produced, and it can be further exploited for obtaining fluorescent molecules with  $\lambda_{exc}$  and  $\lambda_{em}$  more shifted towards the Near-Infrared (NIR) region of the spectrum for a wider application of  $\sigma$  receptor fluorescent ligands in optical molecular imaging techniques.

## Materials and Methods

### Chemistry

Both column chromatography and flash column chromatography were performed with 60 Å pore size silica gel as the stationary phase (1:30 w/w, 63–200  $\mu\text{m}$  particle size, from ICN and 1:15 w/w, 15–40  $\mu\text{m}$  particle size, from Merck respectively). Melting points were determined in open capillaries on a Gallenkamp electrothermal apparatus. Purity of tested compounds was established by combustion analysis, confirming a purity  $\geq 95\%$ . Elemental analyses (C, H, N) were performed on an Eurovector Euro EA 3000 analyzer; the analytical results were within  $\pm 0.4\%$  of the theoretical values unless otherwise indicated.  $^1\text{H}$  NMR spectra were recorded on a Mercury Varian 300 MHz using  $\text{CDCl}_3$  as solvent. The following data were reported: chemical shift ( $\delta$ ) in ppm, multiplicity (s = singlet, d = doublet, t = triplet, m = multiplet), integration and coupling constant(s) in Hertz. Recording of mass spectra was done on an Agilent 6890-5973 MSD gas chromatograph/mass spectrometer and on an Agilent 1100 series LC-MSD trap system VL mass spectrometer; only significant  $m/z$  peaks, with their percentage of relative intensity in parentheses, are reported. Chemicals were from Aldrich and Across and were used without any further purification.

#### 6-(1,4-dioxa-8-azaspiro[4.5]dec-8-yl)hexanenitrile (2)

A mixture of 1,4-dioxa-8-azaspiro[4.5]decane (0.72 mL, 5.6 mmol), triethylamine (0.78 mL, 5.6 mmol) and 6-bromohexanenitrile (0.74 mL, 5.6 mmol) in  $\text{CH}_2\text{Cl}_2$  was stirred at room temperature. The reaction mixture was washed with  $\text{H}_2\text{O}$  and the separated organic layer was concentrated under reduced pressure to give a crude mixture, which was purified by column chromatography with  $\text{CH}_2\text{Cl}_2/\text{MeOH}$  (95:5) as eluent, to afford the target compound as a pale yellow oil (1.16 g, 87% yield):  $^1\text{H}$  NMR  $\delta$  1.42–1.56 (m, 2H), 1.64–1.84 (m, 4H), 1.86–2.10 (m, 4H), 2.36 (t, 2H,  $J = 7.2$  Hz), 2.68 (t, 2H,  $J = 8$  Hz), 2.80–3.00 (m, 4H), 4.00 (s, 4H); GC-MS  $m/z$  239 ( $\text{M}^+ + 1$ , 1), 238 ( $\text{M}^+$ , 3), 156 (100).

#### N-[6-(1,4-dioxa-8-aza-spiro[4.5]dec-8-yl)hexyl]acetamide (3)

A solution of the nitrile **2** (1.0 g, 4.2 mmol) in anhydrous  $\text{Et}_2\text{O}$  (25 mL) was added in a dropwise manner to a suspension of  $\text{LiAlH}_4$  (0.32 g, 8.4 mmol) in the same solvent kept under  $\text{N}_2$  at 0  $^\circ\text{C}$ . The mixture was stirred at 0  $^\circ\text{C}$  for 45 min and then at room temperature overnight.  $\text{H}_2\text{O}$  was carefully added into the reaction pot, and the obtained mixture was filtered on Celite pad, and the filtrate evaporated under reduced pressure to give the corresponding amine as a pale yellow gummy solid (1.0 g, 99% yield); GC-MS  $m/z$  242 ( $\text{M}^+$ , 1), 156 (100). Such amine (1.0 g, 4.2 mmol) was dissolved in anhydrous  $\text{CH}_2\text{Cl}_2$  (40 mL) and added with triethylamine (1.2 mL, 8.6 mmol). Acetyl chloride (0.45 mL, 6.4 mmol) was then dropped at 0  $^\circ\text{C}$ , under  $\text{N}_2$ . The mixture was stirred at room temperature for 3 h, then treated with  $\text{NaHCO}_3$  (sat. solution 20 mL), and extracted with  $\text{CH}_2\text{Cl}_2$  ( $3 \times 20$  mL). The organic layers collected were dried ( $\text{Na}_2\text{SO}_4$ ), and concentrated under reduced pressure to give a crude mixture which was purified by column chromatography with  $\text{CH}_2\text{Cl}_2/\text{MeOH}$

(9:1) as eluent to yield title compound as a pale yellow oil (0.78 g, 66% yield); GC-MS  $m/z$  284 ( $M^+$ , 1), 156 (100).

#### **N-[6-(4-oxopiperidino)hexyl]acetamide (4)**

To a solution of amide **3** (0.32 g, 1.13 mmol) in acetone, 2 N HCl (37 mL) was added and the mixture was heated at reflux for 1 h followed by 1 h at room temperature. The solvent was removed under reduced pressure and conc. NaOH was added to obtain an alkaline pH. The aqueous phase was extracted with AcOEt (3 × 15 mL), the organic layers collected and dried ( $Na_2SO_4$ ) and evaporated under reduced pressure to afford the target compound as a yellow oil (0.17 g, 63% yield) which was used for the next step without further purification;  $^1H$  NMR  $\delta$  1.42-1.84 (m, 8H), 2.10-2.68 (s+m, 13H), 2.90-3.10 (m, 2H), 5.10 (broad s, 1H); GC-MS  $m/z$  240 ( $M^+$ , 1), 112 (100).

#### **6-[4-[4-[3-(5-methoxy-1,2,3,4-tetrahydronaphthalen-1-yl)propyl]piperazin-1-yl]piperidino]hexylamine (6)**

The piperidine **4** (0.16 g, 0.67 mmol) and piperazine **5** (0.19 g, 0.68 mmol) were reacted with  $ZnCl_2$  (0.05 g, 0.39 mmol) and  $NaCNBH_3$  (0.044 g, 0.70 mmol) in 2-propanol (20 mL). The mixture was stirred for 48 h at room temperature. Then, the reaction mixture was evaporated to dryness and the residue was diluted with 2 N NaOH and extracted with AcOEt. The organic layers were washed with brine, dried ( $Na_2SO_4$ ) and then concentrated under reduced pressure to give a crude residue which was purified by column chromatography with  $CH_2Cl_2/MeOH$  (8:2) as eluent to afford the intermediate N-acetyl derivative of compound **6** as a white solid (0.13 g, 39% yield):  $^1H$  NMR 1.20-2.00 (m, 23H), 2.20-2.40 (m, 6H), 2.45-3.00 (m, 14H), 3.20 (m, 2H), 3.80 (s, 3H), 5.45 (broad s, 1H), 6.65 (d, 1H,  $J = 7.7$  Hz), 6.80 (d, 1H,  $J = 7.7$  Hz), 7.08 (t, 1H,  $J = 7.9$  Hz). LC-MS (ESI<sup>+</sup>)  $m/z$  513 [ $M+H$ ]<sup>+</sup>, 535 [ $M+Na$ ]<sup>+</sup>. Such intermediate acetamide (0.22 g, 0.44 mmol) was refluxed in 3N HCl (6.5 mL) for 4 h. After cooling, the mixture was made alkaline with  $K_2CO_3$  (sat. solution, 10 mL) and extracted with  $CH_2Cl_2$  (3 × 10 mL). The collected organic layers were dried ( $Na_2SO_4$ ), and the solvent was evaporated to produce a brown semisolid (0.20 g, 99% yield) which was used for the next step without any further purification.  $^1H$  NMR 1.20-2.00 (m, 20H), 2.20-2.80 (m, 19H), 2.85-3.05 (m, 3H), 3.80 (s, 3H), 5.45 (broad s, 2H,  $D_2O$  exchanged), 6.65 (d, 1H,  $J = 7.7$  Hz), 6.80 (d, 1H,  $J = 7.7$  Hz), 7.08 (t, 1H,  $J = 7.9$  Hz). LC-MS (ESI<sup>+</sup>)  $m/z$  471 [ $M+H$ ]<sup>+</sup>.

#### **2-(6-[5-[3-(4-cyclohexylpiperazin-1-yl)propyl]-5,6,7,8-tetrahydronaphthalen-1-oxo]hexyl)isoindole-1,3-dione (11)**

A grain of NaI,  $K_2CO_3$  (0.14 g, 1.0 mmol) and phthalimide **9** (0.29 g, 1.0 mmol) were added to a solution of phenol **10** (0.26 g, 0.74 mmol) in DMF (5 mL), and the reaction mixture was heated at 100 °C for 18 h. After cooling, the solvent was removed under reduced pressure, then  $H_2O$  (5 mL) was added to the residue and the mixture was extracted with AcOEt (3 × 10 mL). The crude was purified by flash chromatography with ethyl acetate/ $CH_2Cl_2$  (6:4) as eluent to give compound **11** as a yellow oil (0.094g, 16% yield);  $^1H$  NMR  $\delta$  1.21-1.97 (m, 26H), 2.10-2.95 (m, 14H), 3.69 (t, 2H,  $J = 7.2$  Hz), 3.90 (m, 2H), 6.57-7.07 (m, 3H), 7.60-7.86 (m, 4H). LC-MS (ESI<sup>+</sup>)  $m/z$  586 [ $M+H$ ]<sup>+</sup>, 608 [ $M+Na$ ]<sup>+</sup>.

#### **2-[2-[5-[3-(4-Cyclohexylpiperazin-1-yl)propyl]-5,6,7,8-tetrahydronaphthalen-1-oxo]ethoxy]ethanol (12)**

To a solution of phenol **10** (0.14 g, 0.4 mmol) in DMF (5 mL), a grain of NaI,  $K_2CO_3$  (0.06 g, 0.5 mmol) and 2-(2-chloroethoxy)ethanol (0.05 mL, 0.5 mmol) were added, and the reaction mixture was heated at 120 °C for 18 h. After cooling, the solvent was evaporated under reduced pressure, and then water was added to the residue. The mixture was extracted

with AcOEt (3 × 5 mL), and the collected organic layers collected were dried (Na<sub>2</sub>SO<sub>4</sub>) and evaporated to afford a crude which was purified by flash chromatography with AcOEt/CH<sub>2</sub>Cl<sub>2</sub> (7:3) as eluent to give the target compound **12** as a yellow oil (0.11 g, 62% yield); <sup>1</sup>H NMR δ 1.00-1.40 (m, 6H), 1.40-2.00 (m, 12H), 2.40-3.20 (m, 15H), 3.65-3.80 (m, 4H), 3.86-3.90 (m, 2H), 4.06-4.12 (m, 2H), 6.65-7.05 (m, 3H). GC-MS *m/z* 445 (M<sup>+</sup>+1, 5), 444 (M<sup>+</sup>, 22), 181 (100); LC-MS (ESI<sup>+</sup>) *m/z* 445 [M+H]<sup>+</sup>, 467 [M+Na]<sup>+</sup>.

### **2-[2-[2-[5-[3-(4-Cyclohexylpiperazin-1-yl)propyl]-5,6,7,8-tetrahydronaphthalen-1-yloxy]ethoxy]ethyl]isoindole-1,3-dione (13)**

To a stirred solution of alcohol **12** (0.12 g, 0.27 mmol) in dry THF (10 mL) kept under N<sub>2</sub>, triphenylphosphine (0.12 g, 0.46 mmol), phthalimide (0.069 g, 0.47 mmol) and DIAD (0.12 ml, 0.60 mmol) were added and the mixture was stirred at room temperature for 18 h. Then the solvent was evaporated under reduced pressure, the resulting residue was treated with H<sub>2</sub>O and the aqueous layer was extracted with AcOEt (3 × 20 mL). The combined organic layers were dried (Na<sub>2</sub>SO<sub>4</sub>) and concentrated under reduced pressure to give a crude residue which was purified by column chromatography using CH<sub>2</sub>Cl<sub>2</sub>/MeOH (95:5) as eluent, to afford the target compound as a yellow oil (0.10 g, 65% yield); LC-MS (ESI<sup>+</sup>) *m/z* 574 [M+H]<sup>+</sup>, 596 [M+Na]<sup>+</sup>.

### **General Procedure for the Synthesis of 6-[1-[3-(4-cyclohexylpiperazin-1-yl)-propyl]-1,2,3,4-tetrahydronaphthalen-5-yloxy]hexylamine (14) and 2-[2-[1-[3-(4-cyclohexylpiperazin-1-yl)propyl]-1,2,3,4-tetrahydronaphthalen-5-yloxy]ethoxy]ethylamine (15)**

Hydrazine hydrate 50% (0.085 mL, 0.85 mmol) was added to a solution of either **11** or **13** (0.29 mmol) in methanol (3 mL), and the reaction mixture was stirred at room temperature for 30 min. 1.5 N HCl (1.2 mL) was then added and the mixture was stirred for further 12 h. Then 3 N HCl was added until a pH < 2 was obtained, and the mixture was heated at reflux for 30 min. After cooling down to room temperature, the mixture was filtered, the solid residue was washed with cold MeOH and with Et<sub>2</sub>O and dried under vacuum. The white solid obtained was made free base with alkaline treatment to afford the target compound as a pale yellow oil (70% yield).

**6-[1-[3-(4-Cyclohexylpiperazin-1-yl)propyl]-1,2,3,4-tetrahydronaphthalen-5-yloxy]hexylamine (14)**—<sup>1</sup>H NMR δ 1.00-1.30 (m, 5H), 1.40-2.00 (m, 23H), 2.20-2.80 (m, 16H), 3.90 (t, 2H, *J* = 6.0 Hz), 6.60 (d, 1H, *J* = 7.9 Hz), 6.75 (d, 1H, *J* = 7.7 Hz), 7.05 (t, 1H, *J* = 7.9 Hz); LC-MS (ESI<sup>+</sup>) *m/z* 456 [M+H]<sup>+</sup>.

**2-[2-[1-[3-(4-Cyclohexylpiperazin-1-yl)propyl]-1,2,3,4-tetrahydronaphthalen-5-yloxy]ethoxy]ethylamine (15)**—<sup>1</sup>H NMR δ 1.05-1.50 (m, 6H), 1.60-2.10 (m, 12H), 2.40-3.20 (m, 18H), 3.65-3.90 (m, 6H), 6.65-7.05 (m, 3H). LC-MS (ESI<sup>+</sup>) *m/z* 444 [M+H]<sup>+</sup>, 466 [M+Na]<sup>+</sup>.

### **General Procedure for the Synthesis of Final Compounds 7, 16, 17**

4-Chloro-7-nitro-2,1,3-benzoxadiazole (NBD-Cl, 1.0 mmol) was dissolved in absolute EtOH (15 mL) and added in a dropwise manner to one among amines **6**, **14** or **15** (1.0 mmol) dissolved in the same solvent (15 mL). The mixture was stirred for 1.5 h at room temperature. Then, the reaction mixture was filtered and the filtrate evaporated under reduced pressure.



**6-[4-[4-[3-(5-Methoxy-1,2,3,4-tetrahydronaphthalen-1-yl)propyl]piperazin-1-yl]piperidino]-N-(7-nitro-2,1,3-benzoxadiazol-4-yl)hexanamine (7)**

The crude semisolid was purified by column chromatography with AcOEt/MeOH (7:3) as eluent to give the final compound **7** as an orange semisolid (0.26 g, 42% yield); <sup>1</sup>H NMR 1.20-2.20 (m, 21H), 2.25-2.35 (m, 8H), 2.45-2.80 (m, 11H), 3.00-3.10 (m, 2H), 3.20-3.40 (broad s, 1H), 3.80 (s, 3H), 6.18 (d, 1H, *J* = 8.5 Hz), 6.60 (d, 1H, *J* = 7.7 Hz), 6.80 (d, 1H, *J* = 7.7 Hz), 7.05 (t, 1H, *J* = 7.9 Hz), 8.50 (d, 1H, *J* = 8.5 Hz); LC-MS (ESI<sup>+</sup>) *m/z* 634 [M + H]<sup>+</sup>, 656 [M+Na]<sup>+</sup>. Anal. (C<sub>35</sub>H<sub>51</sub>N<sub>7</sub>O<sub>4</sub>·3.8HCl) C, H, N.

**6-[5-[3-(4-Cyclohexylpiperazin-1-yl)propyl]-5,6,7,8-tetrahydronaphthalen-5-yloxy]-N-(7-nitro-2,1,3-benzoxadiazol-4-yl)hexanamine (16)**

The crude semisolid was purified by column chromatography using CH<sub>2</sub>Cl<sub>2</sub>/MeOH (99:1) as eluent to give the target compound **16** as a brown oil (0.37 g, 60% yield); <sup>1</sup>H NMR 1.00-1.40 (m, 10H), 1.50-2.00 (m, 16H), 2.18-2.80 (m, 13H), 3.45-3.55 (m, 3H), 3.94 (t, 2H, *J* = 6.0 Hz), 6.17 (d, 1H, *J* = 8.5 Hz), 6.20-6.30 (broad s, 1H, D<sub>2</sub>O exchanged), 6.60 (d, 1H, *J* = 7.7 Hz), 6.78 (d, 1H, *J* = 7.7 Hz), 7.05 (t, 1H, *J* = 7.9 Hz), 8.50 (d, 1H, *J* = 8.5 Hz). LC-MS (ESI<sup>-</sup>) *m/z* 617 [M-H]<sup>-</sup>. Anal. (C<sub>35</sub>H<sub>50</sub>N<sub>6</sub>O<sub>4</sub>·3HCl·5/4H<sub>2</sub>O) C, H, N.

**2-[2-[5-[3-(4-Cyclohexylpiperazin-1-yl)propyl]-5,6,7,8-tetrahydronaphthalen-1-yloxy]ethoxy]-N-(7-nitro-2,1,3-benzoxadiazol-4-yl)ethanamine (17)**

The crude semisolid was purified by column chromatography using CH<sub>2</sub>Cl<sub>2</sub>/MeOH (99:1) as eluent to give the final compound **17** as a brown oil (0.37 g, 62% yield); <sup>1</sup>H NMR 1.40-2.20 (m, 18H), 2.25-2.80 (m, 14H), 3.50-3.75 (m, 3H), 3.85-4.00 (m, 4H), 4.08-4.15 (m, 2H), 6.17 (d, 1H, *J* = 8.5 Hz), 6.60 (d, 1H, *J* = 7.7 Hz), 6.80 (d, 1H, *J* = 7.7 Hz), 7.05 (t, 1H, *J* = 7.9 Hz), 8.45 (d, 1H, *J* = 8.5 Hz). LC-MS (ESI<sup>+</sup>) *m/z* 607 [M + H]<sup>+</sup>. Anal. (C<sub>33</sub>H<sub>46</sub>N<sub>6</sub>O<sub>5</sub>·3HCl) C, H, N.

**General Procedure for the Synthesis of Final Compounds 8, 18, 19**

A solution of 5-(dimethylamino)naphthalene-1-sulfonyl chloride (dansyl chloride) (0.21 g, 0.8 mmol) in anhydrous CH<sub>2</sub>Cl<sub>2</sub> (15 mL) was added in a dropwise manner to one among amines **6**, **14** or **15** (1.0 mmol) dissolved in the same solvent (15 mL). The mixture was stirred at room temperature for 18 h. Then, the reaction mixture was washed with H<sub>2</sub>O (2 × 30 mL) and the organic phases were collected, dried (Na<sub>2</sub>SO<sub>4</sub>) and evaporated under reduced pressure to afford a crude residue which was purified as described below.

**5-Dimethylamino naphthalene-1-sulfonic acid 6-[4-[4-[3-(5-methoxy-1,2,3,4-tetrahydronaphthalen-1-yl)propyl]piperazin-1-yl]piperidino]hexanamide (8)**

The crude semisolid was purified by column chromatography using CHCl<sub>3</sub>/MeOH (9:1) as eluent to give the target compound as a green oil (0.29 g, 42% yield); <sup>1</sup>H NMR 1.04-1.45 (m, 8H), 1.50-2.10 (m, 12H), 2.20-2.40 (m, 6H), 2.45-2.80 (m, 11H), 2.92-3.02 (m, 11H), 3.80 (s, 3H), 4.90-5.00 (m, 1H D<sub>2</sub>O exchanged), 6.63 (d, 1H, *J* = 7.7 Hz), 6.78 (d, 1H, *J* = 7.7 Hz), 7.08 (t, 1H, *J* = 7.7 Hz), 7.18 (d, 1H, *J* = 7.4 Hz), 7.50-7.60 (m, 2H), 8.22 (d, 1H, *J* = 7.4 Hz), 8.30 (d, 1H, *J* = 7.4 Hz), 8.55 (d, 1H, *J* = 7.4 Hz); LC-MS (ESI<sup>+</sup>) *m/z* 704 [M + H]<sup>+</sup>. Anal. (C<sub>41</sub>H<sub>61</sub>N<sub>5</sub>O<sub>3</sub>S·4HCl·2H<sub>2</sub>O) C, H, N.

**5-Dimethylamino naphthalene-1-sulfonic acid 6-[5-[3-(4-cyclohexylpiperazin-1-yl)propyl]-5,6,7,8-tetrahydronaphthalen-1-yloxy]hexanamide (18)**

The crude semisolid was purified by column chromatography using CH<sub>2</sub>Cl<sub>2</sub>/MeOH (97:3) as eluent to give the target compound **18** as a pale green oil (0.33 g, 48% yield). <sup>1</sup>H NMR 1.00-1.90 (m, 24H), 2.00-2.20 (m, 2H), 2.40-3.10 (m, 22H), 3.80 (t, 2H, *J* = 6 Hz), 4.70-4.80 (m, 1H, D<sub>2</sub>O exchanged), 6.55 (d, 1H, *J* = 7.9 Hz), 6.73 (d, 1H, *J* = 7.7 Hz), 7.00-7.05 (m,

1H), 7.20 (d, 1H,  $J = 7.9$  Hz), 7.50-7.60 (m, 2H), 8.20-8.40 (m, 2H), 8.51 (d, 1H,  $J = 8.5$  Hz); LC-MS (ESI<sup>+</sup>)  $m/z$  689 [M + H]<sup>+</sup>. Anal. (C<sub>41</sub>H<sub>60</sub>N<sub>4</sub>O<sub>3</sub>S·3HCl·3/2H<sub>2</sub>O) C, H, N.

### 5-Dimethylaonaphthalene-1-sulfonic acid 2-[2-[5-[3-(4-cyclohexylpiperazin-1-yl)propyl]-5,6,7,8-tetrahydronaphthalen-5-yloxy]ethoxy]ethanamide (19)

The crude semisolid was purified by column chromatography using CH<sub>2</sub>Cl<sub>2</sub>/MeOH (98:2) as eluent to give the target compound as a pale green oil (0.47 g, 70% yield); <sup>1</sup>H NMR 1.00-2.30 (m, 18H), 2.50-3.40 (m, 22H), 3.45 (t, 2H,  $J = 5$  Hz), 3.55 (t, 2H,  $J = 6$  Hz), 3.90 (t, 2H,  $J = 6$  Hz), 5.20-5.30 (m, 1H, D<sub>2</sub>O exchanged), 6.55 (d, 1H,  $J = 7.9$  Hz), 6.76 (d, 1H,  $J = 7.7$  Hz), 7.00-7.10 (m, 1H), 7.14 (d, 1H,  $J = 7.9$  Hz), 7.40-7.54 (m, 2H), 8.20-8.26 (m, 2H), 8.51 (d, 1H,  $J = 8.5$  Hz); LC-MS (ESI<sup>+</sup>)  $m/z$  677 [M + H]<sup>+</sup>. Anal. (C<sub>39</sub>H<sub>56</sub>N<sub>4</sub>O<sub>4</sub>S·3HCl) C, H, N.

**Fluorescence Spectroscopy and Molar Extinction Coefficient**—Emission spectra of compounds **7**, **8**, **16-19** were determined in EtOH, CHCl<sub>3</sub> and in PBS buffer solution. In all experiments the excitation and the emission bandpass was set at 10 nm. The emission spectra were obtained from 300 to 700 nm with excitation set at the appropriate excitation wavelength. The excitation spectra of compounds **8**, **18**, **19** were obtained from 250 to 450 nm with the emission being recorded at the appropriate wavelength. The excitation spectra of compounds **7**, **16**, **17** were obtained from 300 to 550 nm with the emission being recorded at the appropriate wavelength. Fluorescence quantum yields were calculated with respect to quinine sulfate (Fluka) in 0.5 M H<sub>2</sub>SO<sub>4</sub> as a standard ( $\Phi = 0.546$ ).<sup>41</sup> Solutions of both the sample and the reference were prepared from original solutions diluted with the appropriate solvent so that absorbance was below 0.2 at the same excitation wavelength (347 nm). Fluorescence measurements were carried out for each solution with the same instrument parameters, and the fluorescence spectra were corrected for instrumental response before integration. The quantum yield for each sample was calculated according the following equation:<sup>42</sup>

$$\Phi_x = \Phi_s (A_s/A_x) (F_x/F_s) (n_x/n_s)^2$$

where  $\Phi$  is the emission quantum yield, A is the absorbance at the excitation wavelength, F is the area under the corrected emission curve, n is the refractive index of the solvent for the sample (X) and the standard (S). Absorption spectra were recorded with a PerkinElmer UV-Vis-NIR spectrophotometer, fluorescence spectra were obtained with a PerkinElmer LS55 spectrofluorometer. Molar extinction coefficients ( $\epsilon$ ) were determined for each final compound (**7**, **8**, **16-19**) dissolved in EtOH with concentration ranging from 1  $\mu$ M to 100  $\mu$ M and absorbance spectra recorded from 200 nm to 600 nm in standard quartz cuvettes.  $\epsilon$  Values were determined by fitting the Beer's law:  $A = \epsilon \times c \times d$  where (A) is the absorbance at the  $\lambda_{exc}$ ; (c) is the molar concentration of the solution, and (d) was the optical path length (d = 1 cm). Measurements were repeated twice.

### Biological Methods and Materials: Radioligand Binding Assays

All the procedures for the binding assays were previously described.  $\sigma_1$  And  $\sigma_2$  receptor binding were carried out according to Matsumoto et al.<sup>43</sup> [<sup>3</sup>H]-DTG (30 Ci/mmol) and (+)-[<sup>3</sup>H]-pentazocine (34 Ci/mmol) were purchased from PerkinElmer Life Sciences (Zaventem, Belgium). DTG was purchased from Tocris Cookson Ltd., U.K. (+)-Pentazocine was obtained from Sigma-Aldrich-RBI s.r.l. (Milan, Italy). Male Dunkin guinea-pigs and Wistar Hannover rats (250-300 g) were from Harlan, Italy. The specific radioligands and tissue sources were respectively: (a)  $\sigma_1$  receptor, (+)-[<sup>3</sup>H]-pentazocine (+)-[2S-(2 $\alpha$ ,6 $\alpha$ ,11R)]-1,2,3,4,5,6-hexahydro-6,11-dimethyl-3-(3-methyl-2-butenyl)-2,6-methano-3-

benzazocine-8-ol), guinea-pig brain membranes without cerebellum; (b)  $\sigma_2$  receptor, [ $^3\text{H}$ ]DTG in the presence of 1  $\mu\text{M}$  (+)-pentazocine to mask  $\sigma_1$  receptors, rat liver membranes. The following compounds were used to define the specific binding reported in parentheses: (a) (+)-pentazocine (73-87%), (b) DTG (85-96%). Concentrations required to inhibit 50% of radioligand specific binding ( $\text{IC}_{50}$ ) were determined by using six to nine different concentrations of the drug studied in two or three experiments with samples in duplicate. Scatchard parameters ( $K_d$  and  $B_{\text{max}}$ ) and apparent inhibition constants ( $K_i$ ) values were determined by nonlinear curve fitting, using the Prism, version 3.0, GraphPad software.<sup>44</sup>

**Cell Culture**—BxPC3 pancreatic cancer cells were maintained in Roswell Park Memorial Institute (RPMI) media (GIBCO) supplemented with L-glutamine (2 mM), 4-(2-hydroxyethyl)-1-piperazineethanesulfonic acid (HEPES) (1 mM), pyruvate (1 mM), sodium bicarbonate (0.075% w/v), penicillin and streptomycin (100 IU/mL), amphotericin (0.25  $\mu\text{g}/\text{mL}$ ), and 10% fetal bovine serum (Atlanta Biologicals, Lawrenceville, GA). Cells were seeded at a density of  $2 \times 10^5/\text{mL}$  unless otherwise stated and maintained in a humidified atmosphere of 5%  $\text{CO}_2$  at 37°C.

**Confocal Microscopy**—For sub-cellular compartmentalization, cells grown on glass cover slips were incubated with compound **16** (100 nM) and either ERTracker Red (1  $\mu\text{M}$ ), MitoTracker Red (100 nM), or LysoTracker Red (50 nM) for 30 min at 37 °C. The plasma membrane was visualized using the Vybrant Alexa Fluor 594 Lipid Raft Labeling Kit as directed by the manufacturer. All reagents were obtained from Molecular Probes. Cells were washed with PBS and fixed in 2% paraformaldehyde for 30 min at 37 °C prior to additional washing and mounting to a slide with ProLong Gold antifade reagent. Imaging was performed on a Carl Zeiss Axiovert 100 inverted microscope, fitted with LSM 510 laser scanning microscope camera and software. Images were collected with filter bandwidths corresponding to 505–530 nm for green, 560–615 nm for red, and > 650 nm for far red, with 4 scans over 11.8 sec.

**Internalization of Compound 16 by Flow Cytometry**—To quantify internalization of compound **16**, cells were pretreated with the endocytosis inhibitors phenylarsine oxide (10  $\mu\text{M}$ ) or Filipin III (5  $\mu\text{g}/\text{mL}$ ) for 60 min at 37 °C prior to washing and resuspension in cell media. Compound **16** (25 nM) was added and the mean fluorescence (FL1) quantified with a FACSCalibur flow cytometer (BD Biosciences, San Jose, CA) with kinetic readings over a time period of 60 min. To detect competition of compound **16** with parent and analogous compounds, BxPC3 cells were treated with compounds **1** or **20** at increasing concentrations for 45 min prior to replacement with compound **16** (25 nM) for 45 min at 37 °C and fluorescence intensity quantified by flow cytometry. To deter the influence of cell proliferation by increasing the cell seeding density, BxPC3 cells were seeded at increasing concentrations and the following day, cells were treated with compound **16** (25 nM) for 30 min at 37 °C and fluorescence intensity quantified by flow cytometry.

**Cell Viability**—Sub-cultured BxPC3 cells were seeded at increasing densities from  $1 \times 10^5$  to  $9 \times 10^5$  into 96 well clear bottom plates 24 h prior to treatment with compounds **1** or **20** (100  $\mu\text{M}$ ). Eighteen h later cells were washed with PBS, fixed with 4% paraformaldehyde for 30 min at 37°C, and stained with crystal violet for 15 min at 37 °C. Cells were then washed with PBS and cell density detected with a Bio-Rad Laboratories ChemiDoc XRS+ Imager and quantified with Quantity One software. Viability is represented as the percent density of  $\sigma_2$  agonist treated cells compared to those treated with DMSO vehicle.

## Supplementary Material

Refer to Web version on PubMed Central for supplementary material.

## Acknowledgments

This project was partially financed by Veterans Administration Merit Award (Project 1136919) (WGH), American Cancer Society (Project MRSG08019-01CDD) (WGH), National Institute of Health T32 Training Grant (Project 5T32CA009621-22) (JRH).

## References

1. Quirion R, Bowen WD, Itzhak Y, Junien JL, Musachio JM, Rothman RB, Su T-P, Tam SW, Taylor DP. A proposal for the classification of sigma binding sites. *Trends Pharmacol Sci.* 1992; 13:85–86. [PubMed: 1315463]
2. Hanner M, Moebius FF, Flandorfer A, Knaus HG, Striessnig JM, Kempner E, Glossmann H. Purification, molecular cloning, and expression of the mammalian sigma1-binding site. *Proc Natl Acad Sci U S A.* 1996; 93:8072–8077. [PubMed: 8755605]
3. Tsai S-Y, Hayashi T, Mori T, Su T-P. Sigma-1 receptor chaperones and diseases. *Cent Nerv Syst Agents Med Chem.* 2009; 9:184–189. [PubMed: 20021352]
4. Cobos EJ, Entrena JM, Nieto FR, Cendan CM, Del Pozo E. Pharmacology and therapeutic potential of sigma<sub>1</sub> receptor ligands. *Curr Neuropharmacol.* 2008; 6:344–366. [PubMed: 19587856]
5. Skuza G. Potential antidepressant activity of sigma ligands. *Pol J Pharm.* 2003; 55:923–934.
6. Skuza G, Rogoz Z. Effect of BD1047, a sigma<sub>1</sub> receptor antagonist, in the animal models predictive of antipsychotic activity. *Pharmacol Rep.* 2006; 58:626–635. [PubMed: 17085854]
7. Jansen KL, Faull RL, Storey P, Leslie RA. Loss of sigma binding sites in the CA1 area of the anterior hippocampus in Alzheimer's disease correlates with CA1 pyramidal cell loss. *Brain Res.* 1993; 623:299–302. [PubMed: 8221112]
8. Mishina M, Ishiwata K, Ishii K, Kitamura S, Kimura Y, Kawamura K, Oda K, Sasaki T, Sakayori O, Hamamoto M, Kobayashi S, Katayama Y. Function of sigma<sub>1</sub> receptors in Parkinson's disease. *Acta Neurol Scand.* 2005; 112:103–107. [PubMed: 16008536]
9. Mishina M, Ohyama M, Ishii K, Kitamura S, Kimura Y, Oda K, Kawamura K, Sasaki T, Kobayashi S, Katayama Y, Ishiwata K. Low density of sigma<sub>1</sub> receptors in early Alzheimer's disease. *Ann Nucl Med.* 2008; 22:151–56. [PubMed: 18498028]
10. Matsumoto RR, Gilmore DL, Pouw B, Bowen WD, Williams W, Kausar A, Coop A. Novel analogs of the  $\sigma$  receptor ligand BD1008 attenuate cocaine induced toxicity in mice. *Eur J Pharmacol.* 2004; 492:21–26. [PubMed: 15145701]
11. Kashiwagi H, McDunn JE, Simon PO, Goedegebuure PS, Xu J, Jones L, Chang K, Johnston F, Trinkaus K, Hotchkiss RS, Mach RH, Hawkins WG. Selective sigma-2 ligands preferentially bind to pancreatic adenocarcinomas: applications in diagnostic imaging and therapy. *Mol Cancer.* 2007; 6:48.10.1186/1476-4598-6-48 [PubMed: 17631687]
12. Crawford KW, Bowen WD. Sigma-2 receptor agonists activate a novel apoptotic pathway and potentiate antineoplastic drugs in breast tumor cell lines. *Cancer Res.* 2002; 62:313–322. [PubMed: 11782394]
13. Ostfeld MS, Fehrenbacher N, Hover-Hansen M, Thomsen C, Farkas T, Jaattela M. Effective tumor cell death by sigma-2 receptor ligand siramesine involves lysosomal leakage and oxidative stress. *Cancer Res.* 2005; 65:8975–8983. [PubMed: 16204071]
14. van Waarde A, Rybczynska AA, Ramakrishnan N, Ishiwata K, Elsinga PH, Dierckx RA. Sigma receptors in oncology: therapeutic and diagnostic applications of sigma ligands. *Curr Pharm Des.* 2010; 16:3519–3537. [PubMed: 21050178]
15. Megalizzi V, Le Mercier M, Decaestecker C. Sigma receptors and their ligands in cancer biology: overview and new perspectives for cancer therapy. *Med Res Rev.* 2011; 31 n/a. 10.1002/med.20218

16. Phase I Clinical Trial. ClinicalTrials.gov Identifier: NCT00968656. Assessment of Cellular Proliferation in Tumors by Positron Emission Tomography (PET) Using [ $^{18}\text{F}$ ]ISO-1 (FISO PET/CT).
17. Colabufo NA, Berardi F, Abate C, Contino M, Niso M, Perrone R. Is the  $\sigma_2$  receptor a histone binding protein? *J Med Chem.* 2006; 49:4153–4158. [PubMed: 16821775]
18. Berardi F, Abate C, Ferorelli S, Colabufo NA, Perrone R. 1-Cyclohexylpiperazine and 3,3-dimethylpiperidine derivatives as sigma-1 ( $\sigma_1$ ) and sigma-2 ( $\sigma_2$ ) receptor ligands: a review. *Cent Nerv Syst Agents Med Chem.* 2009; 9:205–219. [PubMed: 20021355]
19. Berardi F, Ferorelli S, Abate C, Colabufo NA, Contino M, Perrone R, Tortorella V. 4-(Tetralin-1-yl)- and 4-(naphthalen-1-yl)alkyl derivatives of 1-cyclohexylpiperazine as  $\sigma$  receptor ligands with agonist  $\sigma_2$  activity. *J Med Chem.* 2004; 47:2308–2317. [PubMed: 15084129]
20. Abate C, Elenewski J, Niso M, Berardi F, Colabufo NA, Azzariti A, Perrone R, Glennon RA. Interaction of the  $\sigma_2$  receptor ligand PB28 with the human nucleosome: computational and experimental probes of interaction with the H2A/H2B dimer. *Chem Med Chem.* 2010; 5:268–273. [PubMed: 20077462]
21. Zeng C, Vangveravong S, Xu J, Chang KC, Hotchkiss RS, Wheeler KT, Shen D, Zhuang Z-P, Kung HF, Mach RH. Subcellular localization of sigma-2 receptors in breast cancer cells using two-photon and confocal microscopy. *Cancer Res.* 2007; 67:6708–6716. [PubMed: 17638881]
22. Zeng C, Vangveravong S, Jones LA, Hyrc K, Chang KC, Xu J, Rothfuss JM, Goldberg MP, Hotchkiss RS, Mach RH. Characterization and evaluation of two novel fluorescent sigma-2 receptor ligands as proliferation probes. *Molecular Imaging.* 2011:1–14.
23. Azzariti A, Colabufo NA, Berardi F, Porcelli L, Niso M, Simone MG, Perrone R, Paradiso A. Cyclohexylpiperazine derivative PB28, a  $\sigma_2$  agonist and  $\sigma_1$  antagonist receptor inhibits cell growth, modulates P-glycoprotein, and synergizes with anthracyclines in breast cancer. *Mol Cancer Ther.* 2006; 5:1807–1816. [PubMed: 16891467]
24. Ferorelli S, Abate C, Colabufo NA, Niso M, Inglese C, Berardi F, Perrone R. Design and evaluation of naphthol- and carbazole-containing fluorescent sigma ligands as potential probes for receptor binding studies. *J Med Chem.* 2007; 50:4648–4655. [PubMed: 17713896]
25. Berardi F, Colabufo NA, Giudice G, Perrone R, Tortorella V, Govoni S, Lucchi L. New  $\sigma$  and 5-HT $_1\text{A}$  receptor ligands:  $\omega$ -(tetralin-1-yl)-n-alkylamine derivatives. *J Med Chem.* 1996; 39:176–182. [PubMed: 8568804]
26. Elslager EF, Moore AM, Short FW, Sullivan JM, Tendick FH. Synthetic amebicides. II. 7-Dialkylaminoalkylbenz[c]acridines and other 7-aminobenz[c]acridines. *JACS.* 1957; 79:4699–4703.
27. Perrone R, Berardi F, Colabufo NA, Leopoldo M, Abate C, Tortorella V. N-Aryl- or N-alkylpiperazine derivatives: the role of N-substituent on  $\sigma_1$ ,  $\sigma_2$ , 5-HT $_1\text{A}$  and D $_2$  receptor affinity. *Med Chem Res.* 2000; 10:201–207.
28. Abate C, Mosier PD, Berardi F, Glennon RA. A structure-affinity and comparative molecular field analysis of sigma-2 ( $\sigma_2$ ) receptor ligands. *Cent Nerv Syst Agents Med Chem.* 2009; 9:246–257. [PubMed: 20021358]
29. Schnitzer JE, Oh P, Pinney E, Allard J. Filipin-sensitive caveolae-mediated transport in endothelium: reduced transcytosis, scavenger endocytosis, and capillary permeability of select macromolecules. *J Cell Biol.* 1994; 127:1217–1232. [PubMed: 7525606]
30. Gibson AE, Noel RJ, Herlihy JT, Ward WF. Phenylarsine oxide inhibition of endocytosis: effects on asialofetuin internalization. *Am J Physiol.* 1989; 257:182–184.
31. Gebreselassie D, Bowen WD. Sigma-2 receptors are specifically localized to lipid rafts in rat liver membranes. *Eur J Pharmacol.* 2004; 493:19–28. [PubMed: 15189760]
32. Torrence-Campbell C, Bowen WD. Differential solubilization of rat liver sigma-1 and sigma-2 receptors: retention of sigma-2 sites in particulate fractions. *Eur J Pharmacol.* 1996; 304:201–210. [PubMed: 8813603]
33. Lajoie P, Nabi IR. Lipid rafts, caveolae, and their endocytosis. *Int Rev Cell Mol Biol.* 2010; 282:135–163. [PubMed: 20630468]
34. Patra SK. Dissecting lipid raft facilitated cell signaling pathways in cancer. *Biochim Biophys Acta.* 2008; 1785:182–206. [PubMed: 18166162]



35. Kashiwagi H, McDunn JE, Simon PO, Goedegebuure PS, Vangveravong S, Chang K, Hotchkiss RS, Mach RH, Hawkins WG. Sigma-2 receptor ligands potentiate chemotherapies and improve survival in models of pancreatic adenocarcinoma. *J Transl Med.* 2009; 7:24.10.1186/1479-5876-7-24 [PubMed: 19323815]
36. Abate C, Niso M, Contino M, Colabufo NA, Ferorelli S, Perrone R, Berardi F. 1-Cyclohexyl-4-(4-arylcyclohexyl)piperazines: mixed  $\sigma$  and human  $\Delta_8$ - $\Delta_7$  Sterol Isomerase ligands with antiproliferative and P-Glycoprotein inhibitory activity. *Chem Med Chem.* 2011; 6:73–80. [PubMed: 21069657]
37. Wheeler KT, Wang LM, Wallen CA, Childers SR, Cline JM, Keng PC, Mach RH. Sigma-2 receptors as a biomarker of proliferation in solid tumours. *Br J Cancer.* 2000; 82:1223–1232. [PubMed: 10735510]
38. Al-Nabulsi I, Mach RH, Wang LM, Wallen CA, Keng PC, Sten K, Childers SR, Wheeler KT. Effect of ploidy, recruitment, environmental factors, and tamoxifen treatment on the expression of sigma-2 receptors in proliferating and quiescent tumour cells. *Br J Cancer.* 1999; 81:925–933. [PubMed: 10576647]
39. Hornick JR, Xu J, Vangveravong S, Tu Z, Mitchem JB, Spitzer D, Goedegebuure P, Mach RH, Hawkins WG. The novel sigma-2 receptor ligand SW43 stabilizes pancreas cancer progression in combination with gemcitabine. *Mol Cancer.* 2010; 9:298. [PubMed: 21092190]
40. Hou C, Tu Z, Mach R, Kung HF, Kung MP. Characterization of a novel iodinated sigma-2 receptor ligand as a cell proliferation marker. *Nucl Med Biol.* 2006; 33:203–209. [PubMed: 16546674]
41. Meech SR, Phillips D. Photophysics of some common fluorescence standards. *J Photochem.* 1983; 23:193–217.
42. Demas JN, Crosby GA. Measurement of photoluminescence quantum yields. A review. *J Phys Chem.* 1971; 75:991–1024.
43. Matsumoto RR, Bowen WD, Tom MA, Truong DD, De Costa BR. Characterization of two novel sigma receptor ligands: antidystonic effects in rats suggest sigma receptor antagonism. *Eur J Pharmacol.* 1995; 280:301–310. [PubMed: 8566098]
44. Prism Software, version 3.0 for Windows. GraphPad Software, Inc.; San Diego, CA: 1998.

## Abbreviations

<b>NBD</b>	7-nitro-1,2,3-benzoxadiazole
<b>ER</b>	endoplasmic reticulum
<b>DIAD</b>	diisopropylazodicarboxylate
<b>SAfIR</b>	Structure–Affinity Relationship
<b>PBS</b>	phosphate buffered saline
<b>PAO</b>	phenylarsine oxide
<b>UV</b>	Ultra-Violet
<b>NIR</b>	Near-Infrared
<b>DMSO</b>	dimethyl sulfoxide

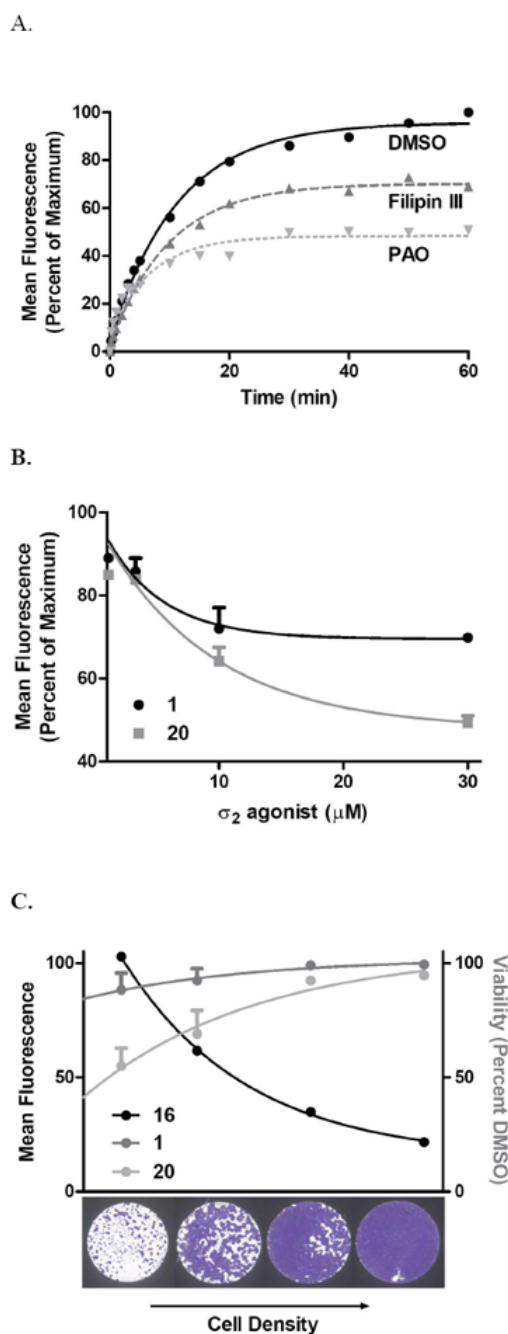


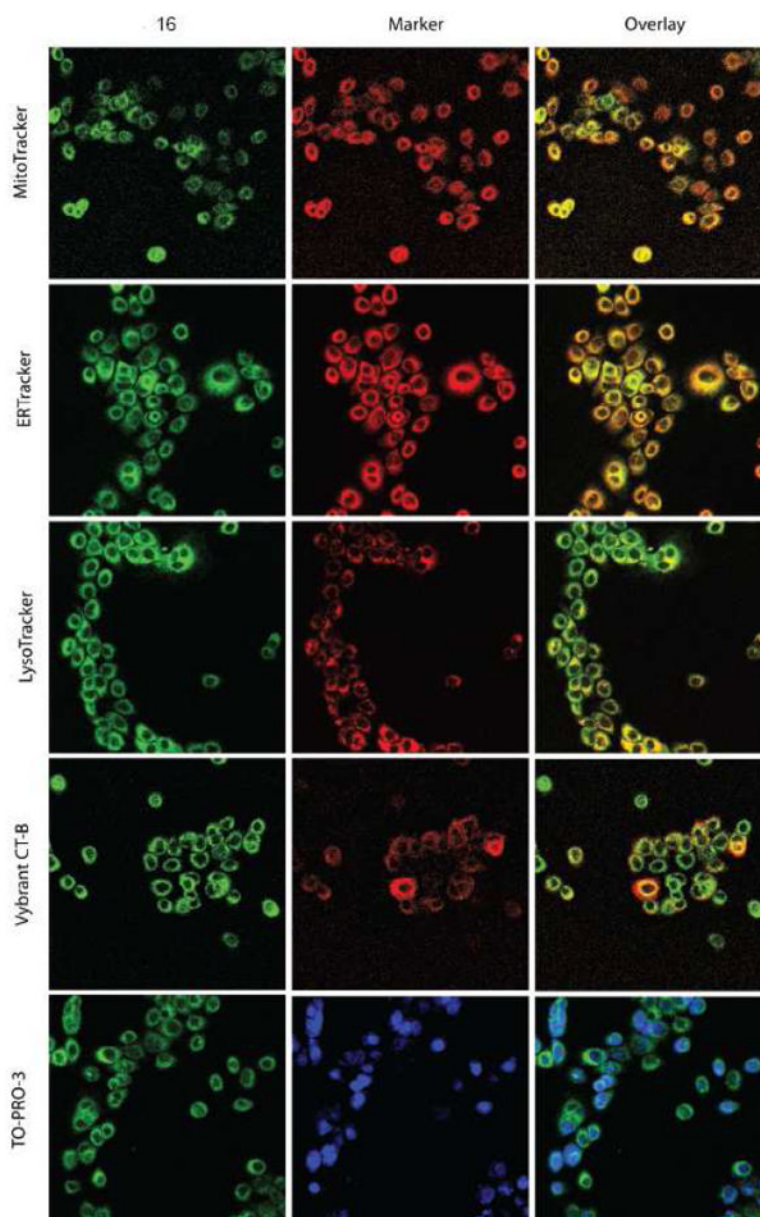
**Figure 1.**

**Cellular Internalization of the Fluorescent  $\sigma_2$  Receptor Ligand **16**.**

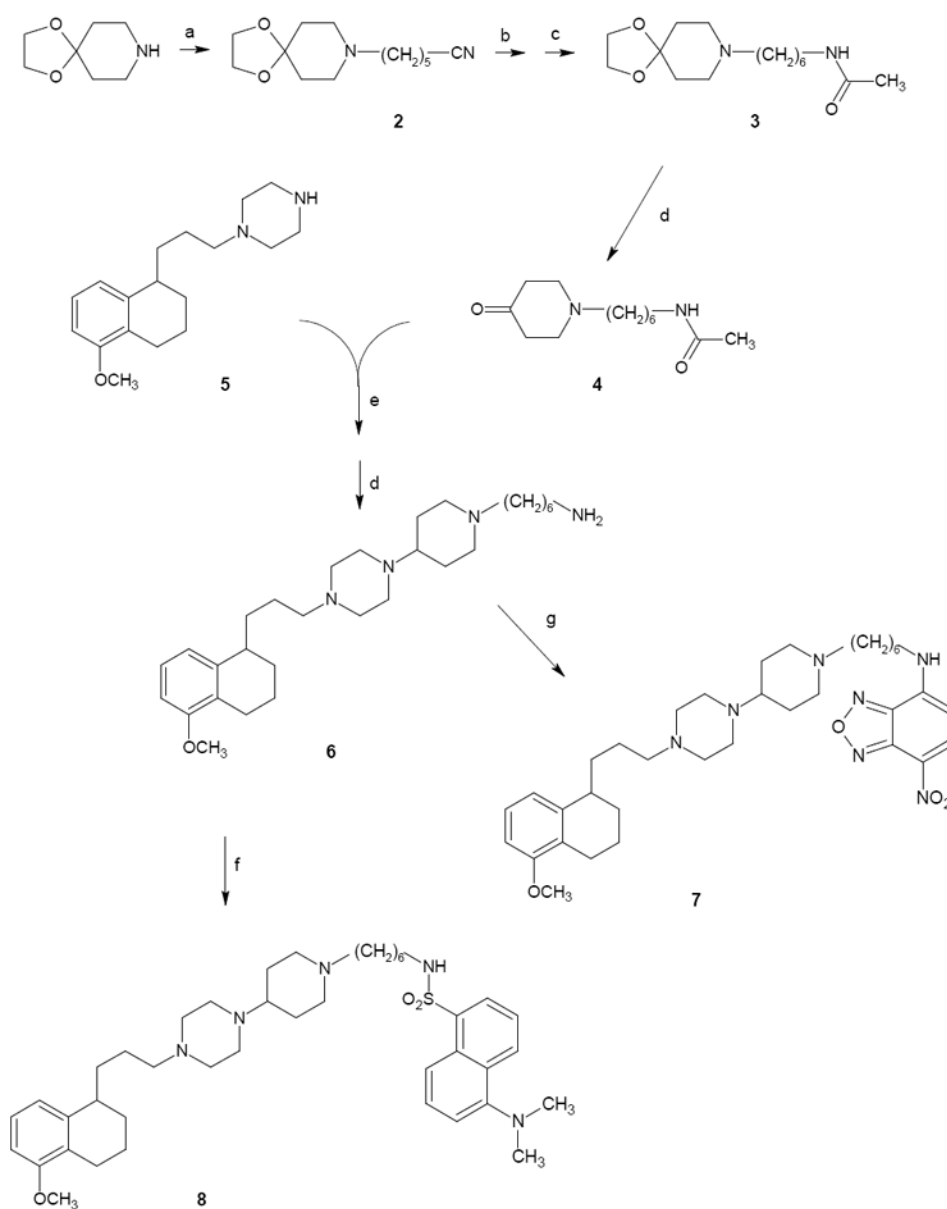
A) Kinetic uptake of compound **16**: BxPC3 pancreatic cancer cells were treated for 1 h with the endocytosis inhibitors Filipin III (5  $\mu\text{g}/\text{mL}$ ) or phenylarsine oxide (PAO, 10  $\mu\text{M}$ ) or DMSO vehicle for 60 min prior to kinetic uptake analysis of **16** (25 nM) by flow cytometry. Compound **16** uptake represents the percentage of the mean fluorescence of maximum signal intensity.

B) Competition of compound **16** by  $\sigma_2$  agonist structural analogs. BxPC3 cells were treated with increasing doses of compounds **1** or **20** for 45 min prior to replacement with compound **16** (25 nM) for 45 min and fluorescence intensity quantified by flow cytometry.

C) Cell density dependence  $\sigma_2$  agonist uptake and cell death. BxPC3 cells were seeded at increasing densities to achieve a range of dividing, subconfluent and quiescent, confluent cultures. The following day, cells were treated with compound **16** (25 nM) and fluorescence intensity quantitated by flow cytometry. Alternatively, cell were treated with compound **1** or **20** (100  $\mu$ M) for 24 hours and viability compared to DMSO control.



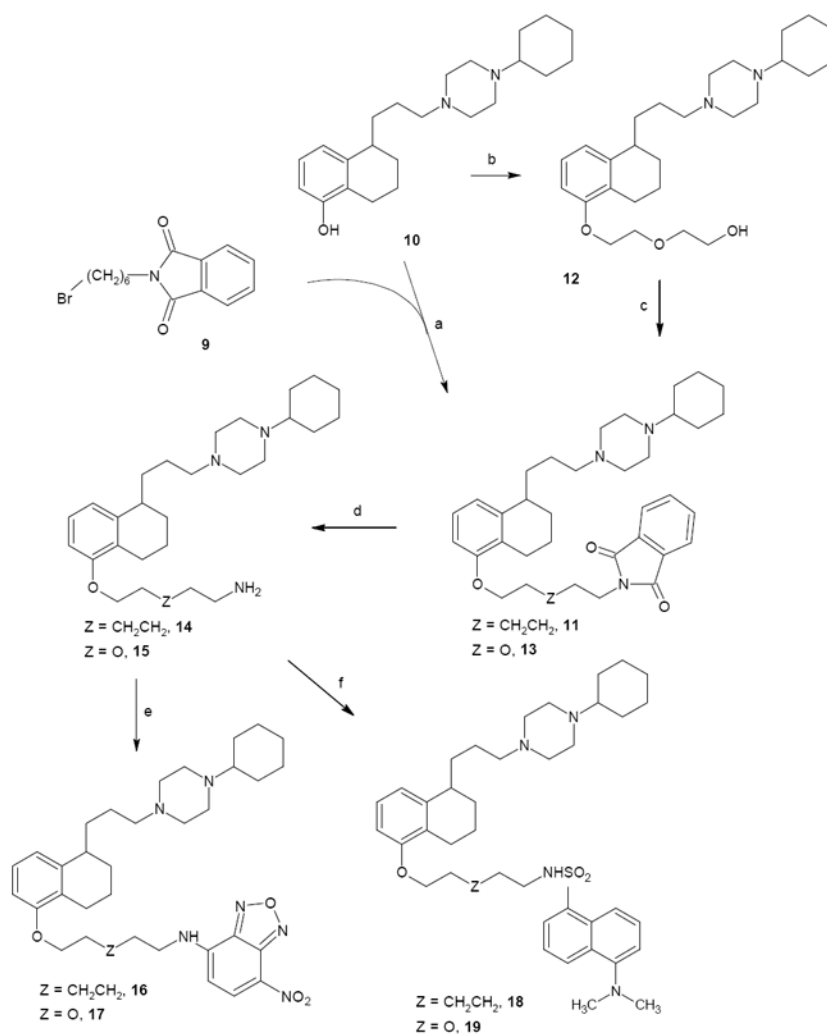
**Figure 2.** Cellular Colocalization of **16** with Subcellular Organelles. BxPC3 pancreatic cancer cells were incubated with **16** and subcellular markers, as described in the Materials and Methods, and imaged by confocal microscopy. **16** is presented as green, organelle markers in red, and overlays in yellow.

**Scheme 1.**

Synthesis of Fluorescent Compound **1** Analogues: fluorescent tag at the piperazine.<sup>a</sup>

<sup>a</sup>Reagents: (a) 6-Br(CH<sub>2</sub>)<sub>5</sub>CN; (b) LiAlH<sub>4</sub>; (c) CH<sub>3</sub>COCl; (d) HCl; (e) ZnCl<sub>2</sub>, NaCNBH<sub>3</sub>; (f) Dansyl chloride; (g) NBD-chloride.



**Scheme 2.**

Synthesis of Fluorescent Compound 1 Analogues: fluorescent tag at the tetralin nucleus.<sup>a</sup>

<sup>a</sup>Reagents: (a)  $\text{K}_2\text{CO}_3$ ; (b)  $\text{ClCH}_2\text{CH}_2\text{OCH}_2\text{CH}_2\text{OH}$ ,  $\text{K}_2\text{CO}_3$ ; (c)  $\text{Ph}_3\text{P}$ , Phthalimide, DIAD; (d) hydrazine hydrate; (e) NBD-chloride; (f) Dansyl chloride.

Table 1

Receptor Affinities and Fluorescence Properties of Final Compounds

comp	X	Y	Z	$K_1$ nM <sup>a</sup>		CHCl <sub>3</sub>		EtOH <sup>b</sup>		PBS <sup>b,c</sup>		$\epsilon^d$		
				$\sigma_1$	$\sigma_2$	$\lambda_{exc}$ nm	$\lambda_{em}$ nm	$\Phi$	$\lambda_{exc}$ nm	$\lambda_{em}$ nm	$\Phi$		$\lambda_{exc}$ nm	$\lambda_{em}$ nm
<b>1</b> <sup>e</sup>	CH <sub>3</sub>	CH <sub>2</sub>		0.38±0.10	0.68±0.20									
<b>7</b>	CH <sub>3</sub>	A	CH <sub>2</sub> CH <sub>2</sub>	2570 <sup>f</sup>	1720±160	450	515	0.17	476	520	0.08	480	535	14391
<b>8</b>	CH <sub>3</sub>	B	CH <sub>2</sub> CH <sub>2</sub>	>5000 <sup>f</sup>	5020±180	346	490	0.32	335	507	0.29	340	510	2600
<b>16</b>	A	CH <sub>2</sub>	CH <sub>2</sub> CH <sub>2</sub>	78.7±18.2	10.8±3.0	451	514	0.20	467	520	0.05	460	520	11300
<b>17</b>	A	CH <sub>2</sub>	O	96.2 <sup>f</sup>	39.3±11.8	450	512	0.18	465	520	0.04	460	520	6544
<b>18</b>	B	CH <sub>2</sub>	CH <sub>2</sub> CH <sub>2</sub>	9.08±1.32	20.8±1.5	340	490	0.30	335	507	0.20	345	485	4000
<b>19</b>	B	CH <sub>2</sub>	O	19.8±8.7	25.7±4.7	345	490	0.48	335	507	0.23	343	510	2741
<b>(+)-pentazocine</b>				2.62±0.25										
<b>DTG</b>					24.6±2.2									

<sup>a</sup> Values are the means of n ≥ 2 separate experiments.<sup>b</sup> Fluorescence properties herein reported were evaluated on compounds as free bases, but they were also evaluated on their corresponding hydrochloride salts in EtOH and PBS solutions. A maximum of 5 nm shift was observed in the excitation and emission wavelengths when compared to the excitation and emission wavelengths from the corresponding free bases.<sup>c</sup> All compounds solubilized in PBS gave  $\Phi$  value very close to 0 and therefore they are not reported.<sup>d</sup> From EtOH solutions of compounds in EtOH.<sup>e</sup> From Ref 18 where results from binding on human cells, in which compound **1** displays about 40-fold  $\sigma_2$  versus  $\sigma_1$  selectivity, are also reported.<sup>f</sup> From a unique experiment.